DTA096A - Lab 1 Report

Visual Representation and Information Theory

Name: Andrea Faccioli
Date: 17/09/2025

1 Experimental Setup

The experiments have been carried out using Python within a Jupyter Notebook environment. Core libraries included NumPy for numerical operations, OpenCV and scikit-image for image processing. All scripts and functions used are provided in Appendix A.2.

2 Visual Representation & Models

2.1 Sampling and Aliasing

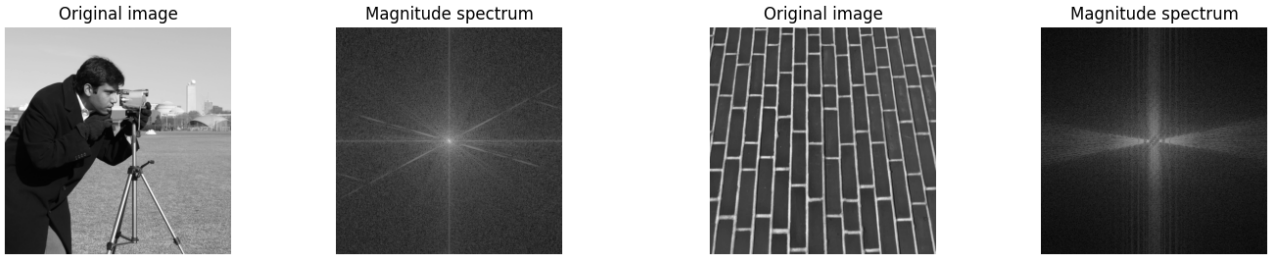

(a) (b)

Figure 1: Smooth image (a) and Textured image (b) with Fourier magnitude spectra

The downsampling experiment clearly showed that without anti-aliasing filters, significant aliasing artifacts and jagged edges. Fourier analysis revealed these resulted from high-frequency (boundaries of spectrum representation) components folding back into the visible spectrum, violating the Nyquist theorem.

Applying Gaussian prefiltering before downsampling markedly reduced aliasing artifacts by attenuating frequencies beyond the new Nyquist limit. The anti-aliased images appeared smoother though with some detail loss, demonstrating the key trade-off in proper sampling between artifact prevention and image sharpness.

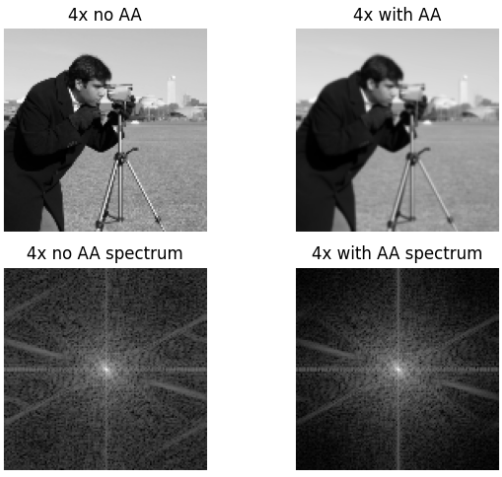

Figure 2: Subsampled images and their magnitude spectrum

Smooth images exhibited minimal aliasing effect, while highly textured images showed pronounced aliasing artifacts with chaotic high-frequency interference patterns due to their abundant spectral content (high-frequencies) exceeding the Nyquist limit.

2.2 Quantization and SQNR

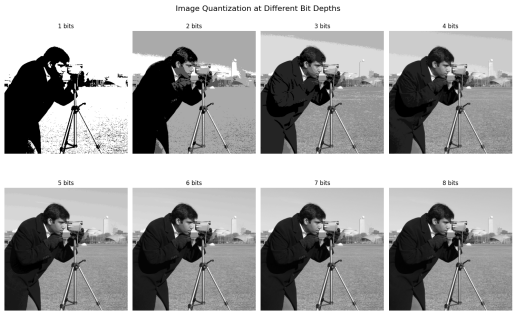

Figure 3: Visualization of an image quantized at 8 different levels

The quantization experiment demonstrated that reducing bit depth introduces visible artifacts and measurable quantization noise, especially in flat and smooth areas, where blocky artifacts are introduced.

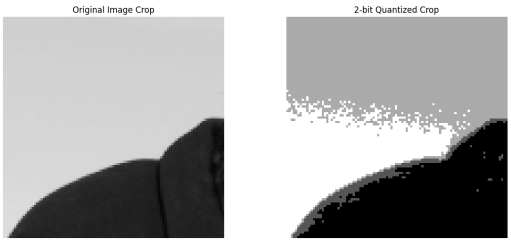

Figure 4: Visualization of a crop of a smooth area

The empirical SQNR curve followed the theoretical 6 dB/bit improvement closely for mid-range bit depths but exhibited extreme deviation at 8 bits, where the MSE approached zero and SQNR diverged to infinity. This occurred because quantizing an already 8-bit image to 8 bits represents an identity operation—the quantization process perfectly reconstructs the original discrete levels, resulting in theoretically zero error.

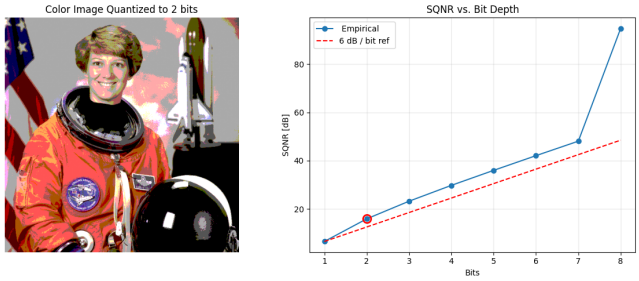

Figure 5: Visualization of color quantized image and SQNR plot

Color image analysis revealed that flat, smooth regions exhibited the most noticeable artifacts in the form of color banding and contouring, while textured areas and edges showed better tolerance to quantization due to their inherent high-frequency content masking the errors.

2.3 Color Models and Chroma Subsampling

Chroma subsampling demonstrates that significant compression can be achieved with minimal perceptual quality loss by exploiting the human visual system's reduced sensitivity to color detail compared to luminance information.

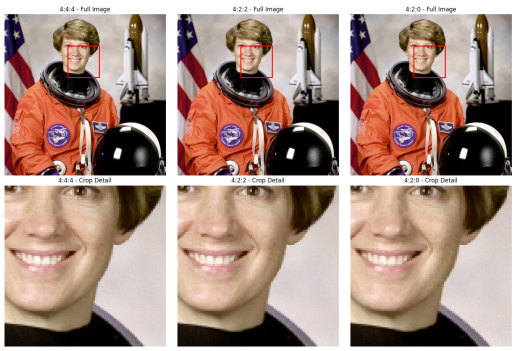

Figure 6: Chroma subsampling results and cropped tiles.

The technique proves most effective in smooth regions like skin tones and skies, where chroma information changes gradually, while detailed textures and sharp color edges show the most visible artifacts, particularly in the form of color bleeding and loss of fine chromatic details.

3 Information Theory for Images

3.1 Entropy of Simple Sources

Distribution	**Entropy (bits)**
Fair die (H_f)	2.585
Biased die (H_b)	2.522
Joint entropy of two fair dice (H_{xy})	5.170
Sum of individual fair dice entropies ($H_f + H_f$)	5.170

Table 1: Entropy values for different dice distributions

The entropy calculations demonstrate that the fair die (2.585 bits) has higher uncertainty than the biased die (2.522 bits), confirming that more predictable distributions yield lower entropy. The joint entropy of two fair dice (5.170 bits) exactly equals the sum of their individual entropies (2.585 + 2.585 = 5.170 bits), indicating these are independent events with no shared information.

3.2 Image Entropy and Histograms

The analysis of two complementary images clearly demonstrate that the textured grass image (7.29 bits) has significantly higher entropy than the smooth moon image (4.89 bits), indicating it contains more information and uncertainty in its pixel values. This difference arises because the grass image's complex texture produces a more uniform distribution of gray values, while the moon image's smoother surfaces concentrate around fewer intensity levels.

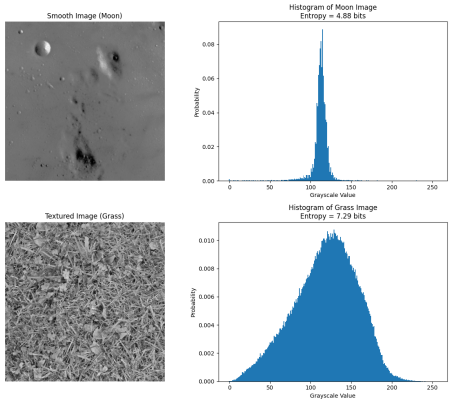

Figure 7: Smooth vs Textured image histograms

Consequently, the moon image has greater compression potential as its lower entropy suggests more predictable pixel patterns that can be efficiently encoded. The textured grass image, with its higher entropy, will be less compressible since its pixel values are more random and less predictable, requiring more bits to represent the image without loss.

3.3 Joint and Conditional Entropy

The analysis of the Moon image from scikit-image reveals strong spatial dependencies between adjacent pixels. The conditional entropy $H(Y|X) = 2.26$ bits is significantly lower than the marginal entropy $H(Y) = 4.89$ bits, demonstrating that knowing a pixel's value substantially reduces uncertainty about its neighbor. This predictability is quantified by the mutual information $I(X;Y) = 2.62$ bits, indicating that approximately 2.62 bits of information are shared between adjacent pixels.

Information Measure	**Value (bits)**
Marginal Entropy $H(X)$	4.8851
Marginal Entropy $H(Y)$	4.8854
Joint Entropy $H(X,Y)$	7.1488
Conditional Entropy $H(Y\|X)$	2.2637
Mutual Information $I(X;Y)$	2.6213

Table 2: Information theory measures for adjacent pixels in the Moon image

These results confirm that natural images contain substantial spatial redundancy, where neighboring pixels are highly correlated rather than independent. This predictability forms the theoretical foundation for lossless image compression techniques, as the conditional entropy represents the minimum bitrate needed to encode the image when exploiting spatial correlations, which is substantially lower than what would be required treating each pixel as independent.

3.4 Predictive Coding and Redundancy

The predictive coding implementation demonstrates a substantial reduction in entropy from 4.8850 bits in the original image to just 1.9121 bits in the residual image, achieving a coding gain of approximately 3 bits per pixel. This significant reduction confirms that spatial predictors effectively exploit the correlations between neighboring pixels, capturing the predictable components of the image and leaving behind a residual with much lower information content.

Metric	**Value**
Original Image Entropy ($H(X)$)	4.8850 bits
Residual Image Entropy ($H(R)$)	1.9121 bits
Redundancy (R)	0.3894

Table 3: Predictive coding results for the Moon image

The calculated redundancy value of R = 0.3894 quantifies the proportion of "wasted" information in the original representation, indicating that nearly 39% of the bits in a classical encoding would be redundant.

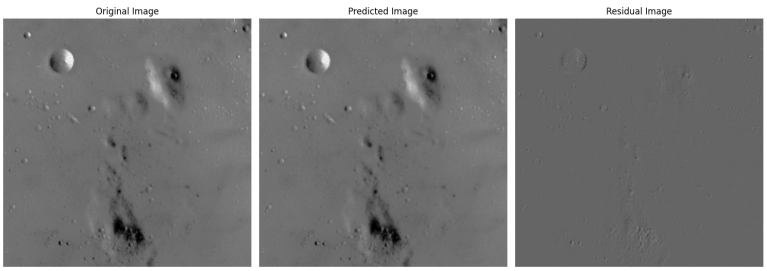

Figure 8: Predicted and residual image

A Appendix 1a

A.1 Images collection

The images processed in Lab 1 session here.

A.2 Source code

The complete code of Lab 1 session can be found here.